

Expected Harmonics (Version 1.0) in BNL-built LHC Dipoles

A. Jain

January 1998

Collider Accelerator Department
Brookhaven National Laboratory

U.S. Department of Energy

USDOE Office of Science (SC), High Energy Physics (HEP) (SC-25)

Notice: This technical note has been authored by employees of Brookhaven Science Associates, LLC under Contract No. DE-AC02-76CH00016 with the U.S. Department of Energy. The publisher by accepting the technical note for publication acknowledges that the United States Government retains a non-exclusive, paid-up, irrevocable, world-wide license to publish or reproduce the published form of this technical note, or allow others to do so, for United States Government purposes.

DISCLAIMER

This report was prepared as an account of work sponsored by an agency of the United States Government. Neither the United States Government nor any agency thereof, nor any of their employees, nor any of their contractors, subcontractors, or their employees, makes any warranty, express or implied, or assumes any legal liability or responsibility for the accuracy, completeness, or any third party's use or the results of such use of any information, apparatus, product, or process disclosed, or represents that its use would not infringe privately owned rights. Reference herein to any specific commercial product, process, or service by trade name, trademark, manufacturer, or otherwise, does not necessarily constitute or imply its endorsement, recommendation, or favoring by the United States Government or any agency thereof or its contractors or subcontractors. The views and opinions of authors expressed herein do not necessarily state or reflect those of the United States Government or any agency thereof.

Expected Harmonics (Version 1.0) in BNL-built LHC Dipoles

Animesh K. Jain

RHIC Project, Brookhaven National Laboratory, Upton, New York 11973-5000

1. Introduction

It is proposed to build several types of dipoles for the Large Hadron Collider (LHC) at BNL. All these dipoles require a coil inner diameter of 8 cm and will use the same coil design that was used for the RHIC arc dipoles (DRG type). The beam separations at the D4A and D4B locations are 234 mm and 194 mm respectively, which are smaller than the outer diameter (266.7 mm) of the yoke in the DRG magnets. As a result, these magnets must be built as twin-aperture magnets with redesigned yokes. Such yokes have been designed [1] employing a $550 \text{ mm} \times 659.2 \text{ mm}$ oblate shape. The beam separations at the D3A and D3B magnet locations are 400 mm and 382 mm respectively. These magnets also can be built as twin-aperture magnets using yokes of the same dimensions as for the D4A and D4B magnets [1]. However, it may be more cost effective to build these magnets as single aperture magnets, identical to the DRG magnets. As an added advantage, the horizontal size of the D4A and D4B yokes can be reduced somewhat, without giving up field quality. A preliminary design has been carried out for D4A and D4B yokes with a vertical size of 550 mm and a reduced horizontal size of 625 mm [2].

The expected field quality for the $550 \text{ mm} \times 659.2 \text{ mm}$ yoke design is given in reference [1]. This note describes the field quality expected in the DRG and $550 \text{ mm} \times 625 \text{ mm}$ magnet designs under conditions of LHC operation. For the single aperture magnets which will be identical to the RHIC dipoles, the expected numbers are based entirely on measured data in DRG magnets. The presence of a second cold mass nearby as well as asymmetric placement of the cold masses in the cryostat will result in some change in the unallowed harmonics at high fields. These effects are not included at present in the numbers for the single aperture "DRG-Like" magnets. For the twin-aperture D4A and D4B magnets, the field quality estimates are based on data in the DRG magnets, as well as numerical calculations. At present, these calculations include the effect of cross-talk between the two apertures, but do not include the effect of the cryostat. One quadrant of the cold mass for the DRG, D4A and D4B magnets (preliminary) is shown in Fig. 1.

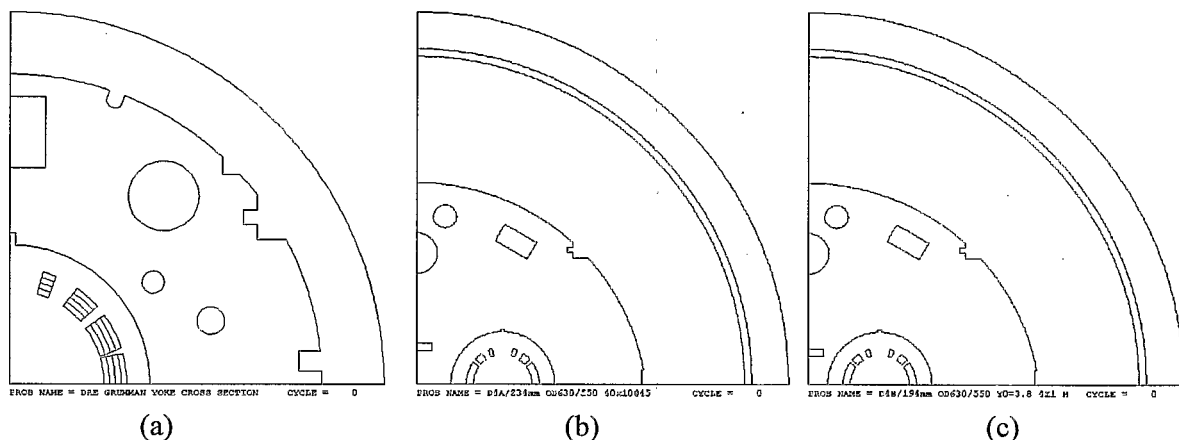


Fig.1 One quadrant of the cold mass in the (a) DRG, (b) D4A and (c) D4B dipoles. The D4A and D4B designs are with a $550 \text{ mm} \times 625 \text{ mm}$ yoke. The placement of bus slots etc. is tentative.

2. Procedure for Estimating Field Quality

In view of the vast amount of experimental data available on the DRG/DR8 magnets, it is relatively straightforward to estimate the field quality in “DRG-Like” magnets at any current. The field quality in the D4A and D4B magnets is also expected to be similar at low fields, since all magnets employ the same RHIC coil design. In particular, warm (room temperature) measurements of harmonics are insensitive to details of the yoke design, persistent currents, and iron saturation. Therefore, DRG, D4A and D4B magnets should have similar harmonic content when warm. The statistical distributions of these harmonics are well known from warm measurements in 296 RHIC dipoles.

In order to obtain the expected straight section harmonics at any given current in the superconducting state, one should add the following contributions to the warm straight section harmonics:

- a) The effect of cool down, i.e., any systematic change in harmonics due to a change in geometry upon cool down. Ideally, this should be zero.
- b) The effect of persistent currents in an “Up Ramp”. This is most notable at injection, but may not be negligible even at high fields.
- c) The current dependence of harmonics, i.e., change in harmonics due to iron saturation, deformation of the coil due to Lorentz forces, etc.

The integral harmonics at any current can be obtained by adding the contribution of ends to the estimated straight section harmonics. Since the ends of the coils are expected to be the same as the RHIC dipoles, the end harmonics are also well known. The following sections provide more details on the estimation of the various contributions mentioned above.

2.1 The effect of cool down

Ideally, one expects the magnet to retain its shape as it cools down from room temperature to liquid helium temperature. In practice, there may be some systematic deformations that would lead to a systematic difference between the harmonics measured warm and the *geometric* harmonics measured cold at sufficiently low fields. The warm harmonics in all the 9.45 m long RHIC dipoles (DRG and DR8 types) were measured using 10 axial positions of a 1 m long rotating coil. In 55 of these magnets, cold harmonics were measured at the 5th position by carrying out a DC loop between 50A and 6000A (~4 T). Harmonics are measured both during an “Up Ramp” and a “Down Ramp” of the current. The current is ramped to a given value at 16 A/s, and is then held constant during these measurements, which begin 15 seconds after the end of the ramp. These data, therefore, do not contain any contribution from eddy currents due to the ramps, but do contain the effect of persistent currents. The geometric values of harmonics can be obtained by averaging the “Up Ramp” and the “Down Ramp” values at sufficiently low fields, where the yoke iron is not saturated. A comparison of this geometric value with the warm measurement at position 5 gives the warm-cold difference.

Fig. 2 shows the correlation between the geometric sextupole terms measured warm and cold at position 5 in 55 DRG/DR8 magnets. The cold values are obtained by averaging the “Up Ramp” and the “Down Ramp” data at 1800A (1.275 T). The same results are obtained by choosing any other current between 500 A and 2000 A. The solid line in Fig. 2 represents a perfect agreement between the warm and the cold values. As seen from Fig. 2, there is an excellent agreement between the skew sextupole terms (open triangles) measured warm and cold. However, the normal sextupole term measured cold differs from the warm value by -0.944 unit on an average with a standard deviation of 0.20 unit. In comparison, the mean warm-cold offset of the skew sextupole is 0.034 unit with a standard deviation of 0.10 unit. The small offset for the skew term shows that the systematic offset in the normal term is a genuine effect and is not due to calibration differences in the two measurement

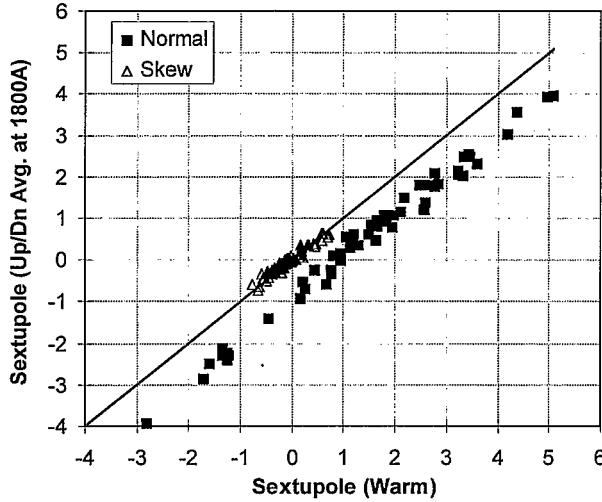


Fig.2 Correlation between the normal (filled squares) and skew (open triangles) sextupole terms measured warm and cold at the same straight section location in 55 DRG/DR8 magnets.

Table I
Changes in harmonics on cool down
(in "units" at 2.5 cm reference radius)

n^*	Δb_n	Δa_n
2	-0.22	0.53
3	-0.94	0.03
4	-0.01	0.02
5	0.04	0.01
6	0.00	0.00
7	-0.05	0.01
8	-0.01	-0.01
9	-0.01	-0.01
10	0.04	0.03
11	-0.02	-0.01

[* $n = 2$ denotes the quadrupole term]

systems. Similar plots were used to obtain the systematic warm-cold differences in other harmonics. The results are summarized in Table I.

2.2 The effect of persistent currents

The harmonics measured cold are offset from the geometric values due to the presence of persistent currents in the coil. Nominally, the persistent currents also have a dipole symmetry. As a result, only the allowed terms such as the normal sextupole, the normal decapole, etc. are affected in a significant way. The direction of persistent currents is reversed during the "Down Ramp" measurements. Hence, the contribution from these currents can be estimated by taking half of the difference between the "Up Ramp" and the "Down Ramp" harmonics measured at the same current.

The magnet current required for LHC injection field of 0.2 T is ~300 A in these dipoles. Both "Up Ramp" and "Down Ramp" data are available at this current in the DRG magnets. Fig. 3 shows the correlation between the "Down Ramp" and "Up Ramp" values of the sextupole terms measured at

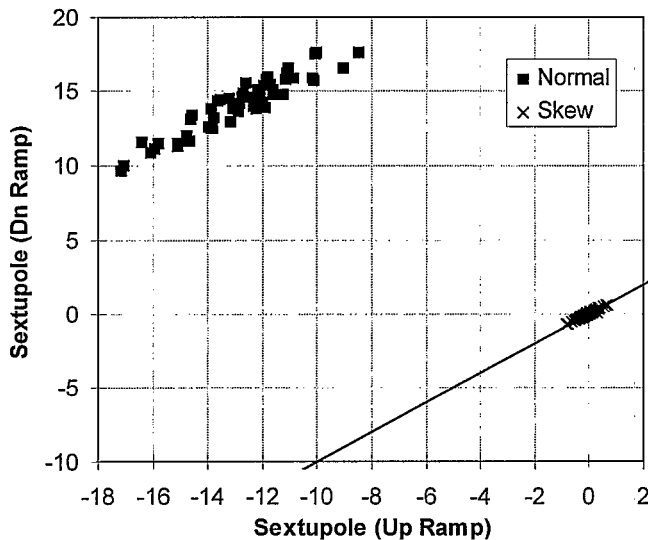


Fig.3 Correlation between the sextupole terms measured at 300A during the "Up Ramp" and the "Down Ramp" of a DC loop at a straight section position in DRG/DR8 dipoles. The values are in units at 2.5 cm reference radius. The solid line represents the case of no difference between the two measurements.

300 A in the DRG/DR8 magnets. As expected, the unallowed skew sextupole (crosses) shows no hysteresis, whereas the normal sextupole measured in the “Down Ramp” is higher than the “Up Ramp” value by 26.90 units on an average. The standard deviation in the “Up-Down difference” is 0.66 unit. In comparison, the mean up-down difference for the skew sextupole term is 0.04 unit with a standard deviation of 0.05 unit. The up-down differences for all the harmonics were obtained in a similar way at each current of interest. Half the value of these differences represent the contribution from persistent currents to the harmonics in the “Up Ramp”. The results are given in Table II for “DRG-Like” magnets at 300A (0.21 T), 5200A (3.52 T) and 5800A (3.85 T).

In the case of the D4A and the D4B magnets, the distribution of persistent currents is expected to be the same, since these magnets also employ the same RHIC coil design. However, these magnets have a collared coil, unlike the DRG magnets where the yoke itself serves as the collar. The yoke inner radius is thus larger in these magnets. This has the effect of pushing the image currents further away. The harmonics due to persistent currents in these magnets will therefore be slightly smaller than the DRG magnets at the same dipole field. For a given current distribution, the amplitude of the $2n$ -pole term, $C(n)$, depends on the mean coil radius, a , and the yoke inner radius, R_{yoke} , according to the following relation (assuming infinite outer radius, with no saturation)

$$C(n) \propto \left[1 + \left(\frac{\mu - 1}{\mu + 1} \right) \left(\frac{a}{R_{yoke}} \right)^{2n} \right] \quad (1)$$

The mean radius of the RHIC dipole coil is 4.5 cm and R_{yoke} is 5.969 cm in DRG magnets and 7.08 cm in the D4A and D4B magnets. Knowing the strengths of various harmonics from persistent currents in the DRG magnets (see Table II), one can estimate the strengths for the D4A and D4B magnets using Eq. (1). The results are given in Table III for various dipole field strengths. The effect due to a different yoke inner radius is at the level of a few percent, and mainly affects the normal sextupole at injection.

As can be seen from Tables II and III, the effect of persistent currents is practically zero for all the unallowed terms. The small effect in the quadrupole terms at injection field could be a genuine effect, or could be due to feed down from the large sextupole terms as a result of small errors (~ 0.2 mm) in centering of the data. At higher fields, the effect of persistent currents is reduced considerably, and practically vanishes for all terms except the normal sextupole.

Table II Differences between “Down Ramp” and “Up Ramp” harmonics measured in “DRG-Like” magnets. The harmonics are at 2.5 cm reference radius.

n ($n=2$ is quadrupole)	$b_n(\text{Dn}) - b_n(\text{Up})$			$a_n(\text{Dn}) - a_n(\text{Up})$		
	300A (0.21 T)	5200A (3.52 T)	5800A (3.85 T)	300A (0.21 T)	5200A (3.52 T)	5800A (3.85 T)
2	-0.51	-0.01	-0.01	-0.51	-0.08	-0.01
3	26.90	1.04	0.58	0.04	0.01	0.00
4	-0.02	0.00	0.00	0.15	-0.05	-0.01
5	0.61	0.01	0.04	0.00	0.00	0.00
6	-0.05	0.00	0.00	-0.07	0.00	0.00
7	0.96	0.03	0.03	0.00	0.00	0.00
8	0.02	0.00	0.00	0.02	0.00	0.00
9	-0.19	0.00	0.00	0.00	0.00	0.00
10	-0.02	0.00	0.00	-0.03	0.00	0.00
11	0.25	0.01	0.00	0.00	0.00	0.00

Table III Estimated values of differences between “Down Ramp” and “Up Ramp” harmonics in D4A and D4B magnets. The estimates are based on measured hysteresis at the nearest current in DRG/DR8 magnets and Eq. (1). The harmonics are at 2.5 cm reference radius.

n ($n = 2$ is quadrupole)	$b_n(\text{Dn}) - b_n(\text{Up})$			$a_n(\text{Dn}) - a_n(\text{Up})$		
	315A (0.20 T)	5610A (3.55 T)	6015A (3.80 T)	315A (0.20 T)	5610A (3.55 T)	6015A (3.80 T)
2	-0.45	-0.01	0.00	-0.45	-0.03	0.00
3	24.22	0.69	0.12	0.04	0.00	0.00
4	-0.02	0.00	0.00	0.14	-0.02	0.00
5	0.58	0.03	0.00	0.00	0.00	0.00
6	-0.05	0.00	0.00	-0.07	0.00	0.00
7	0.95	0.03	0.01	0.00	0.00	0.00
8	0.02	0.00	0.00	0.02	0.00	0.00
9	-0.19	0.00	0.00	0.00	0.00	0.00
10	-0.02	0.00	0.00	-0.03	0.00	0.00
11	0.25	0.00	0.00	0.00	0.00	0.00

2.3 Current dependence of harmonics

In addition to the effect of the persistent currents, the harmonics show a dependence on current at high fields due to saturation of the yoke iron, deformation of the coil by Lorentz forces, etc. All such effects can be lumped together, and the overall current dependence will be referred to as “saturation” of the harmonics. At low fields, there should be no change from the geometric values. In practice, the “true” saturation effect can be obtained by studying the average of up and down ramp harmonics as a function of current, as shown in Fig. 4 for the magnet DRG200. The “saturation induced” harmonics in DRG-Like magnets can be obtained from such plots. The results are given in Table IV. Since these measurements are with a single cold mass, the effect of cross-talk from another cold mass placed nearby (e.g. in the D3A and D3B magnets) is not included. Such an effect will be included in later versions of the expected harmonics in these magnets. Also, the as-measured skew

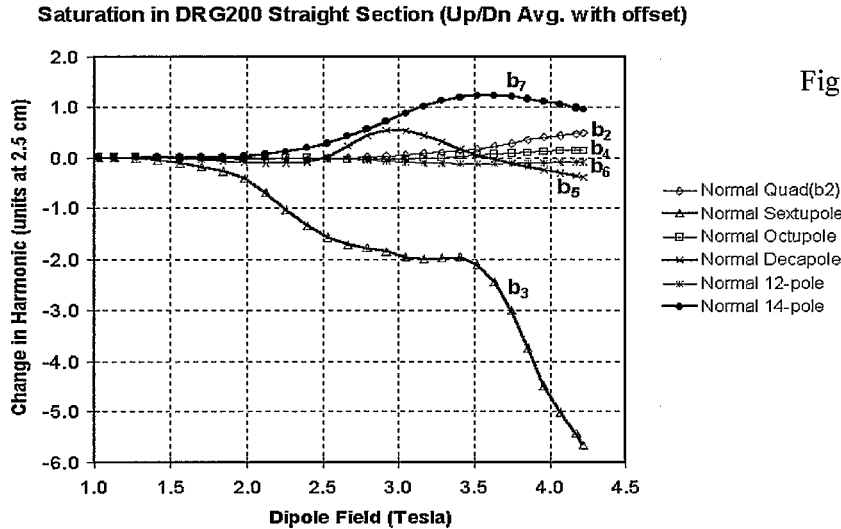


Fig. 4 Current dependence of some of the harmonics in DRG200. The “Up” and “Down” ramp values of the harmonics are averaged to obtain these plots. The geometric values at low fields (~1.0 T) are made zero for each harmonic by using appropriate offsets.

Table IV Deviations of *geometric* harmonics in “DRG-Like” magnets from mid-field values. The values are based on measurements in DRG200 at position 5, and are at 2.5 cm radius. The effect of another cold mass nearby, or of the cryostat, is not included (see text).

n ($n = 2$ is quadrupole)	Change in b_n (units)			Change in a_n (units)		
	300A (0.21 T)	5200A (3.52 T)	5800A (3.85 T)	300A (0.21 T)	5200A (3.52 T)	5800A (3.85 T)
2	−0.06	0.17	0.34	−0.64	0.00	0.00
3	0.45	−2.10	−3.74	0.00	−0.20	−0.24
4	−0.03	0.05	0.11	0.19	0.00	0.00
5	0.45	0.05	−0.19	−0.01	−0.02	−0.02
6	−0.02	−0.13	−0.12	−0.07	−0.06	−0.05
7	0.17	1.23	1.16	0.01	0.00	0.00
8	−0.01	0.00	0.00	0.00	0.00	0.00
9	0.05	−0.01	0.01	0.01	0.00	0.00
10	−0.01	0.01	0.01	−0.03	0.01	0.01
11	0.02	−0.03	−0.04	0.00	0.00	0.00

quadrupole and skew octupole terms show significant saturation due to asymmetric placement of the cold mass in the cryostat. However, this effect depends strongly on the actual weights of the upper and the lower yoke halves, and varies significantly from magnet to magnet. The nominal values for these effects should be estimated using the appropriate cryostat configuration. Such an estimation has not been carried out at present. Consequently, the values for “saturation” in these harmonics are set to zero in Table IV.

The saturation behaviour of twin-aperture D4A and D4B magnets at high fields will be different from the DRG magnets due to entirely different yoke designs. No experimental data are available yet on these magnets. At injection, the small current dependence observed in DRG magnets (see Table IV) should also apply to the D4A and D4B magnets. At high fields, the behaviour of harmonics in these magnets has been estimated using POISSON models shown in Fig. 1(b) and (c). While these calculations should predict the effect of yoke saturation quite reliably, any deformation due to Lorentz forces is not included. Therefore, the actual current dependence in these magnets may differ from such estimates. Nevertheless, in the absence of measured data, the calculations provide the best estimates of current dependence. As can be seen from the models in Fig. 1, the cross talk due to two apertures in the D4A and D4B magnets is included in the calculations, but any top-bottom asymmetry (due to

Table V Deviations of *geometric* harmonics in D4A and D4B magnets from low-field values. The values are based on POISSON calculations. A top-bottom asymmetry due to the cryostat is not included in these calculations.

	D4A Magnets		D4B Magnets	
	5610A (3.55 T)	6015A (3.80 T)	5612A (3.55 T)	6020A (3.80 T)
b_2	0.17	0.14	0.14	0.02
b_3	0.21	0.03	−0.02	−0.27
b_4	−0.01	−0.03	−0.10	−0.17
b_5	−0.31	−0.53	−0.24	−0.40
b_6	0.00	0.00	−0.02	−0.04
b_7	0.02	0.02	0.02	0.04

the cryostat) is not included. With these models, only the normal harmonics will show a current dependence and no saturation in the skew terms is expected. The results of POISSON calculations are summarized in Table V for the D4A and D4B designs. As can be seen from Table V, all harmonics are expected to have negligible current dependence in these designs. The control of saturation has been achieved by a 40 mm \times 10 mm slot located at a suitable position in the yoke.

3. Estimation of “Uncertainty in the Mean” and the “Standard Deviation”

The mean values of warm harmonics in all the magnets employing the same RHIC coil are expected to be the same as the RHIC dipoles, and are easily obtainable from the data. However, in a new production run, the mean values may differ somewhat from the RHIC dipoles due to use of new parts, tooling, etc., which may be within the allowable tolerance, yet may be systematically different from those used in the production of RHIC dipoles. This introduces an uncertainty in the mean value itself, which will be referred to as $\Delta\langle b_n \rangle$ and $\Delta\langle a_n \rangle$ for the normal and skew terms. Theoretically, one could estimate such an uncertainty from the allowed tolerances in the dimensions of various critical parts and the sensitivities of various harmonics to these dimensions. However, such an approach is cumbersome and often leads to an overestimation of the errors. In practice, errors due to various parts tend to cancel each other. In the rare event that errors from all parts are cumulative, the harmonics will become so large that one would almost certainly take some corrective action (such as adjustments in the midplane and pole shims) to bring the mean closer to the expected values.

A more practical approach to estimating the uncertainty in the mean is to look at the distribution of various harmonics in the production run of RHIC dipoles. Assuming that the parts used in all the RHIC dipoles represent a reasonable ensemble of all the possible combinations of errors in various parts, the uncertainty in the mean value of any harmonic should roughly be the same as the maximum deviation of that harmonic from the mean in the RHIC dipoles. In other words, the mean value of any harmonic in a new production batch could possibly lie anywhere between the maximum and the minimum values observed in the DRG/DR8 dipoles. Accordingly, the values of $\Delta\langle b_n \rangle$ and $\Delta\langle a_n \rangle$ quoted in this note are obtained from the maximum deviation from mean observed in DRG/DR8 magnets at 660A for values at injection, and at 5000A for values at high fields. One may argue that magnets near tail of a distribution should be ignored for this purpose, which would lead to slightly smaller uncertainties. On the other hand, the actual uncertainty may be slightly more at high fields due to inaccuracies in predicting the saturation behaviour.

The standard deviation in any harmonic results from random errors in the dimensions of various parts used, as well as random errors during other production steps. These random errors in the production of LHC dipoles are expected to be of the same order as in the RHIC dipole production. As a result, a reliable estimate of the standard deviation in any harmonic [denoted by $\sigma(b_n)$ and $\sigma(a_n)$] can simply be obtained from the standard deviation in the RHIC production. For values at injection, the standard deviation values at 660A are used, whereas for high field values, data at 5000A are used.

4. Expected Values of Straight Section Harmonics

The starting point for the mean values of all the harmonics in all the magnet types is the warm measurements data in DRG/DR8 magnets. Since all LHC dipoles to be built by BNL will use the same RHIC coil design, the warm harmonics are expected to be the same in all these dipoles. These harmonics are known, and are summarized in Table VI. In view of a cross section change at production sequence number 106, only dipoles with sequence number 106 and above are included for

Table VI. Mean values of body harmonics measured warm in DRG/DR8 magnets

$n \rightarrow$	2	3	4	5	6	7	8	9	10	11
b_n	0.15	0.26	-0.02	0.45	-0.01	-0.02	0.00	0.03	0.00	-0.52
a_n	0.06	-0.09	0.00	-0.06	0.00	-0.02	0.00	-0.01	0.00	0.00

obtaining the allowed terms (b_3 , b_5 , b_7 , ...). This change did not affect the unallowed terms. Consequently, all magnets are included to obtain the mean values for the unallowed terms.

The expected values for the straight section harmonics in any particular LHC dipole at any excitation can be obtained by adding the contributions from the warm-cold effect, the persistent currents and any “saturation” or current dependence. All these contributions are described in detail in Sec. 2. The estimated values of straight section harmonics at dipole field strengths of 0.2 T, 3.55 T and 3.80 T in “DRG-Like”, D4A and D4B dipoles are given in Tables VII-IX. The values of the uncertainty in the mean [$\Delta(b_n)$ and $\Delta(a_n)$] and the standard deviation [$\sigma(b_n)$ and $\sigma(a_n)$] are based on DRG/DR8 data at 660A or 5000A, as described in Sec. 3, and are the same for all styles of dipoles.

Table VII. Expected values of body harmonics in “DRG-Like” magnets

A. Body harmonics at 0.2 T in “DRG-Like” magnets (Ver. 1.0)

n	$\langle b_n \rangle$	$\Delta(b_n)$	$\sigma(b_n)$	$\langle a_n \rangle$	$\Delta(a_n)$	$\sigma(a_n)$
2	0.12	0.75	0.28	0.20	4.13	1.56
3	-13.68	5.43	1.98	-0.07	0.51	0.19
4	-0.05	0.23	0.09	0.14	1.18	0.41
5	0.63	0.85	0.42	-0.05	0.18	0.06
6	0.00	0.10	0.03	-0.03	0.54	0.16
7	-0.39	0.22	0.10	0.00	0.07	0.03
8	-0.03	0.04	0.01	-0.01	0.15	0.05
9	0.17	0.13	0.05	0.00	0.03	0.01
10	0.04	0.06	0.02	0.02	0.05	0.02
11	-0.64	0.05	0.02	-0.01	0.02	0.01

B. Body harmonics at 3.55 T in “DRG-Like” magnets (Ver. 1.0)

n	$\langle b_n \rangle$	$\Delta(b_n)$	$\sigma(b_n)$	$\langle a_n \rangle$	$\Delta(a_n)$	$\sigma(a_n)$
2	0.10	0.80	0.28	0.63	3.47	1.55
3	-3.30	3.43	1.82	-0.26	0.58	0.21
4	0.01	0.25	0.09	0.04	1.08	0.42
5	0.53	0.81	0.41	-0.07	0.19	0.06
6	-0.14	0.12	0.04	-0.05	0.56	0.17
7	1.14	0.20	0.11	-0.01	0.07	0.03
8	-0.01	0.04	0.01	-0.01	0.15	0.05
9	0.01	0.12	0.05	-0.01	0.03	0.01
10	0.05	0.06	0.02	0.04	0.04	0.02
11	-0.57	0.04	0.02	-0.01	0.02	0.01

C. Body harmonics at 3.8 T in “DRG-Like” magnets (Ver. 1.0)

n	$\langle b_n \rangle$	$\Delta(b_n)$	$\sigma(b_n)$	$\langle a_n \rangle$	$\Delta(a_n)$	$\sigma(a_n)$
2	0.28	0.80	0.28	0.60	3.47	1.55
3	-4.72	3.43	1.82	-0.30	0.58	0.21
4	0.07	0.25	0.09	0.02	1.08	0.42
5	0.28	0.81	0.41	-0.07	0.19	0.06
6	-0.13	0.12	0.04	-0.05	0.56	0.17
7	1.07	0.20	0.11	-0.01	0.07	0.03
8	-0.01	0.04	0.01	-0.01	0.15	0.05
9	0.03	0.12	0.05	-0.02	0.03	0.01
10	0.05	0.06	0.02	0.04	0.04	0.02
11	-0.58	0.04	0.02	-0.01	0.02	0.01

Table VIII. Expected values of body harmonics in D4A magnets

A. Body harmonics at 0.2 T in D4A magnets (Ver. 1.0)

n	$\langle b_n \rangle$	$\Delta(b_n)$	$\sigma(b_n)$	$\langle a_n \rangle$	$\Delta(a_n)$	$\sigma(a_n)$
2	0.09	0.75	0.28	0.17	4.13	1.56
3	-12.34	5.43	1.98	-0.07	0.51	0.19
4	-0.05	0.23	0.09	0.14	1.18	0.41
5	0.65	0.85	0.42	-0.05	0.18	0.06
6	0.00	0.10	0.03	-0.03	0.54	0.16
7	-0.38	0.22	0.10	0.00	0.07	0.03
8	-0.03	0.04	0.01	-0.01	0.15	0.05
9	0.17	0.13	0.05	0.00	0.03	0.01
10	0.04	0.06	0.02	0.02	0.05	0.02
11	-0.64	0.05	0.02	-0.01	0.02	0.01

B. Body harmonics at 3.55 T in D4A magnets (Ver. 1.0)

n	$\langle b_n \rangle$	$\Delta(b_n)$	$\sigma(b_n)$	$\langle a_n \rangle$	$\Delta(a_n)$	$\sigma(a_n)$
2	0.11	0.80	0.28	0.60	3.47	1.55
3	-0.82	3.43	1.82	-0.06	0.58	0.21
4	-0.04	0.25	0.09	0.03	1.08	0.42
5	0.16	0.81	0.41	-0.05	0.19	0.06
6	-0.01	0.12	0.04	0.00	0.56	0.17
7	-0.07	0.20	0.11	-0.01	0.07	0.03
8	-0.01	0.04	0.01	-0.01	0.15	0.05
9	0.02	0.12	0.05	-0.01	0.03	0.01
10	0.04	0.06	0.02	0.04	0.04	0.02
11	-0.54	0.04	0.02	-0.01	0.02	0.01

C. Body harmonics at 3.8 T in D4A magnets (Ver. 1.0)

n	$\langle b_n \rangle$	$\Delta(b_n)$	$\sigma(b_n)$	$\langle a_n \rangle$	$\Delta(a_n)$	$\sigma(a_n)$
2	0.07	0.80	0.28	0.59	3.47	1.55
3	-0.71	3.43	1.82	-0.05	0.58	0.21
4	-0.06	0.25	0.09	0.02	1.08	0.42
5	-0.04	0.81	0.41	-0.05	0.19	0.06
6	-0.01	0.12	0.04	0.00	0.56	0.17
7	-0.05	0.20	0.11	-0.01	0.07	0.03
8	-0.01	0.04	0.01	-0.01	0.15	0.05
9	0.02	0.12	0.05	-0.01	0.03	0.01
10	0.04	0.06	0.02	0.04	0.04	0.02
11	-0.54	0.04	0.02	-0.01	0.02	0.01

Table IX. Expected values of body harmonics in D4B magnets

A. Body harmonics at 0.2 T in D4B magnets (Ver. 1.0)

n	$\langle b_n \rangle$	$\Delta(b_n)$	$\sigma(b_n)$	$\langle a_n \rangle$	$\Delta(a_n)$	$\sigma(a_n)$
2	0.09	0.75	0.28	0.17	4.13	1.56
3	-12.34	5.43	1.98	-0.07	0.51	0.19
4	-0.05	0.23	0.09	0.14	1.18	0.41
5	0.65	0.85	0.42	-0.05	0.18	0.06
6	0.00	0.10	0.03	-0.03	0.54	0.16
7	-0.38	0.22	0.10	0.00	0.07	0.03
8	-0.03	0.04	0.01	-0.01	0.15	0.05
9	0.17	0.13	0.05	0.00	0.03	0.01
10	0.04	0.06	0.02	0.02	0.05	0.02
11	-0.64	0.05	0.02	-0.01	0.02	0.01

B. Body harmonics at 3.55 T in D4B magnets (Ver. 1.0)

n	$\langle b_n \rangle$	$\Delta(b_n)$	$\sigma(b_n)$	$\langle a_n \rangle$	$\Delta(a_n)$	$\sigma(a_n)$
2	0.08	0.80	0.28	0.60	3.47	1.55
3	-1.05	3.43	1.82	-0.06	0.58	0.21
4	-0.13	0.25	0.09	0.03	1.08	0.42
5	0.23	0.81	0.41	-0.05	0.19	0.06
6	-0.03	0.12	0.04	0.00	0.56	0.17
7	-0.07	0.20	0.11	-0.01	0.07	0.03
8	-0.01	0.04	0.01	-0.01	0.15	0.05
9	0.02	0.12	0.05	-0.01	0.03	0.01
10	0.04	0.06	0.02	0.04	0.04	0.02
11	-0.54	0.04	0.02	-0.01	0.02	0.01

B. Body harmonics at 3.8 T in D4B magnets (Ver. 1.0)

n	$\langle b_n \rangle$	$\Delta(b_n)$	$\sigma(b_n)$	$\langle a_n \rangle$	$\Delta(a_n)$	$\sigma(a_n)$
2	-0.04	0.80	0.28	0.59	3.47	1.55
3	-1.02	3.43	1.82	-0.05	0.58	0.21
4	-0.21	0.25	0.09	0.02	1.08	0.42
5	0.08	0.81	0.41	-0.05	0.19	0.06
6	-0.05	0.12	0.04	0.00	0.56	0.17
7	-0.04	0.20	0.11	-0.01	0.07	0.03
8	-0.01	0.04	0.01	-0.01	0.15	0.05
9	0.02	0.12	0.05	-0.01	0.03	0.01
10	0.04	0.06	0.02	0.04	0.04	0.02
11	-0.54	0.04	0.02	-0.01	0.02	0.01

5. Expected Values of Lead and Return End Harmonics

The lead end and return end harmonics in DRG/DR8 magnets were determined using data from 10 positions of a 1 m long rotating coil. These harmonics, expressed in unit.m (normalized to the central dipole field), have been found to have the same value in warm, as well as cold measurements at low to intermediate fields. At high fields, there is a small saturation effect seen, particularly in the normal sextupole term. Since the end design for all the BNL-built LHC dipoles will be the same as for the DRG/DR8 magnets, the end harmonics in all these dipoles are also expected to be the same. Tables X and XI summarize the expected values for the lead and return end harmonics. The values at 0.2 T are taken from DRG/DR8 data at 660A (0.47 T) and those at 3.55/3.80 T are from data at 5000A (3.4 T).

Table X. Expected values of **lead end** harmonics in all BNL-built LHC dipoles

A. Lead end harmonics (in unit.m) at 0.2 T (Ver. 1.0)

n	$\langle b_n \rangle$	$\Delta(b_n)$	$\sigma(b_n)$	$\langle a_n \rangle$	$\Delta(a_n)$	$\sigma(a_n)$
2	-0.33	2.16	0.96	-2.39	4.24	1.67
3	18.90	2.83	1.06	-9.93	1.00	0.39
4	0.05	0.72	0.22	-0.12	0.76	0.27
5	-0.26	0.70	0.21	2.26	0.31	0.13
6	0.00	0.25	0.11	-0.02	0.31	0.09
7	1.06	0.11	0.05	-0.83	0.13	0.06
8	0.00	0.06	0.02	-0.01	0.07	0.03
9	-0.06	0.06	0.02	0.24	0.05	0.02
10	-0.01	0.07	0.02	-0.01	0.05	0.02
11	-0.06	0.03	0.01	-0.04	0.03	0.01

B. Lead end harmonics (in unit.m) at 3.55 T/3.80 T (Ver. 1.0)

n	$\langle b_n \rangle$	$\Delta(b_n)$	$\sigma(b_n)$	$\langle a_n \rangle$	$\Delta(a_n)$	$\sigma(a_n)$
2	-0.47	2.26	0.99	-1.42	4.27	1.77
3	22.35	2.93	1.10	-9.85	1.01	0.39
4	0.04	0.73	0.23	0.09	0.75	0.29
5	-0.43	0.69	0.22	2.23	0.30	0.13
6	0.02	0.29	0.12	0.01	0.29	0.10
7	0.92	0.11	0.05	-0.86	0.13	0.06
8	0.00	0.06	0.03	-0.02	0.08	0.03
9	-0.04	0.08	0.03	0.25	0.05	0.02
10	-0.01	0.08	0.03	-0.01	0.04	0.02
11	-0.06	0.03	0.01	-0.04	0.02	0.01

Table XI. Expected values of **return end** harmonics in all BNL-built LHC dipoles

A. Return end harmonics (in unit.m) at 0.2 T (Ver. 1.0)

n	$\langle b_n \rangle$	$\Delta(b_n)$	$\sigma(b_n)$	$\langle a_n \rangle$	$\Delta(a_n)$	$\sigma(a_n)$
2	0.24	1.93	0.66	-0.34	4.58	1.68
3	3.95	2.41	1.06	0.26	1.04	0.33
4	0.01	0.34	0.15	0.00	0.68	0.29
5	0.18	0.57	0.22	-0.01	0.31	0.11
6	-0.02	0.15	0.05	-0.03	0.21	0.08
7	0.06	0.13	0.06	-0.03	0.12	0.04
8	-0.03	0.08	0.03	-0.02	0.11	0.04
9	-0.17	0.07	0.03	0.00	0.04	0.02
10	-0.07	0.08	0.04	-0.02	0.10	0.05
11	-0.12	0.03	0.01	0.01	0.02	0.01

B. Return end harmonics (in unit.m) at 3.55 T/3.80 T (Ver. 1.0)

n	$\langle b_n \rangle$	$\Delta(b_n)$	$\sigma(b_n)$	$\langle a_n \rangle$	$\Delta(a_n)$	$\sigma(a_n)$
2	0.22	1.81	0.66	0.91	4.50	1.91
3	6.08	2.67	1.16	0.29	1.03	0.34
4	0.00	0.36	0.16	0.24	0.73	0.31
5	0.03	0.66	0.23	0.00	0.31	0.11
6	0.03	0.17	0.06	-0.01	0.24	0.10
7	-0.04	0.13	0.06	-0.03	0.12	0.05
8	-0.03	0.07	0.03	-0.02	0.11	0.04
9	-0.17	0.08	0.03	0.00	0.05	0.02
10	-0.07	0.08	0.04	-0.02	0.10	0.05
11	-0.12	0.04	0.01	0.01	0.02	0.01

6. Expected Values of Integral Harmonics

The expected values of the integral harmonics can be obtained by adding the contribution of the ends to the straight section. To obtain this contribution in “units”, one must divide the values of end harmonics in unit.m (Tables X and XI) by the magnetic length, L . The measured value of L in DRG/DR8 magnets is 9.43 m at low fields (cold) and 9.44 m at high fields. Using these values for the magnetic length, the integral harmonics are given in Tables XII to XIV. As in the case of the body and end harmonics, the uncertainty in the mean and the standard deviation are determined from the data at 600A for the injection field and at 5000A for higher fields.

Table XII. Expected values of integral harmonics in “DRG-Like” magnets

A. Integral harmonics at 0.2 T in “DRG-Like” magnets (Ver. 1.0)

n	$\langle b_n \rangle$	$\Delta(b_n)$	$\sigma(b_n)$	$\langle a_n \rangle$	$\Delta(a_n)$	$\sigma(a_n)$
2	0.11	0.77	0.28	-0.09	3.68	1.53
3	-11.26	5.52	1.95	-1.10	0.49	0.17
4	-0.05	0.20	0.08	0.12	1.15	0.42
5	0.62	0.83	0.40	0.18	0.16	0.06
6	-0.01	0.08	0.03	-0.03	0.54	0.15
7	-0.27	0.21	0.10	-0.09	0.07	0.02
8	-0.03	0.03	0.01	-0.01	0.15	0.05
9	0.14	0.13	0.04	0.02	0.03	0.01
10	0.03	0.05	0.02	0.02	0.05	0.02
11	-0.66	0.04	0.02	-0.01	0.02	0.01

B. Integral harmonics at 3.55 T in “DRG-Like” magnets (Ver. 1.0)

n	$\langle b_n \rangle$	$\Delta(b_n)$	$\sigma(b_n)$	$\langle a_n \rangle$	$\Delta(a_n)$	$\sigma(a_n)$
2	0.08	0.79	0.28	0.57	3.71	1.51
3	-0.29	3.57	1.70	-1.27	0.55	0.18
4	0.01	0.21	0.08	0.07	1.08	0.41
5	0.49	0.80	0.39	0.17	0.17	0.06
6	-0.13	0.10	0.04	-0.05	0.55	0.16
7	1.23	0.19	0.10	-0.11	0.06	0.02
8	-0.01	0.03	0.01	-0.01	0.15	0.05
9	-0.01	0.12	0.04	0.01	0.03	0.01
10	0.04	0.05	0.02	0.04	0.04	0.02
11	-0.59	0.04	0.02	-0.01	0.01	0.01

C. Integral harmonics at 3.8 T in “DRG-Like” magnets (Ver. 1.0)

n	$\langle b_n \rangle$	$\Delta(b_n)$	$\sigma(b_n)$	$\langle a_n \rangle$	$\Delta(a_n)$	$\sigma(a_n)$
2	0.25	0.79	0.28	0.54	3.71	1.51
3	-1.71	3.57	1.70	-1.31	0.55	0.18
4	0.07	0.21	0.08	0.06	1.08	0.41
5	0.24	0.80	0.39	0.16	0.17	0.06
6	-0.12	0.10	0.04	-0.05	0.55	0.16
7	1.17	0.19	0.10	-0.11	0.06	0.02
8	-0.02	0.03	0.01	-0.01	0.15	0.05
9	0.01	0.12	0.04	0.01	0.03	0.01
10	0.04	0.05	0.02	0.04	0.04	0.02
11	-0.60	0.04	0.02	-0.01	0.01	0.01

Table XIII. Expected values of integral harmonics in D4A magnets

A. Integral harmonics at 0.2 T in D4A magnets (Ver. 1.0)

n	$\langle b_n \rangle$	$\Delta(b_n)$	$\sigma(b_n)$	$\langle a_n \rangle$	$\Delta(a_n)$	$\sigma(a_n)$
2	0.08	0.77	0.28	-0.12	3.68	1.53
3	-9.92	5.52	1.95	-1.10	0.49	0.17
4	-0.05	0.20	0.08	0.13	1.15	0.42
5	0.64	0.83	0.40	0.18	0.16	0.06
6	-0.01	0.08	0.03	-0.03	0.54	0.15
7	-0.26	0.21	0.10	-0.09	0.07	0.02
8	-0.03	0.03	0.01	-0.01	0.15	0.05
9	0.14	0.13	0.04	0.02	0.03	0.01
10	0.03	0.05	0.02	0.02	0.05	0.02
11	-0.66	0.04	0.02	-0.01	0.02	0.01

B. Integral harmonics at 3.55 T in D4A magnets (Ver. 1.0)

n	$\langle b_n \rangle$	$\Delta(b_n)$	$\sigma(b_n)$	$\langle a_n \rangle$	$\Delta(a_n)$	$\sigma(a_n)$
2	0.08	0.79	0.28	0.55	3.71	1.51
3	2.19	3.57	1.70	-1.07	0.55	0.18
4	-0.04	0.21	0.08	0.06	1.08	0.41
5	0.12	0.80	0.39	0.19	0.17	0.06
6	0.00	0.10	0.04	0.00	0.55	0.16
7	0.02	0.19	0.10	-0.11	0.06	0.02
8	-0.01	0.03	0.01	-0.01	0.15	0.05
9	0.00	0.12	0.04	0.01	0.03	0.01
10	0.03	0.05	0.02	0.03	0.04	0.02
11	-0.56	0.04	0.02	-0.01	0.01	0.01

C. Integral harmonics at 3.8 T in D4A magnets (Ver. 1.0)

n	$\langle b_n \rangle$	$\Delta(b_n)$	$\sigma(b_n)$	$\langle a_n \rangle$	$\Delta(a_n)$	$\sigma(a_n)$
2	0.05	0.79	0.28	0.53	3.71	1.51
3	2.30	3.57	1.70	-1.07	0.55	0.18
4	-0.06	0.21	0.08	0.05	1.08	0.41
5	-0.08	0.80	0.39	0.19	0.17	0.06
6	-0.01	0.10	0.04	0.00	0.55	0.16
7	0.04	0.19	0.10	-0.10	0.06	0.02
8	-0.01	0.03	0.01	-0.01	0.15	0.05
9	0.00	0.12	0.04	0.01	0.03	0.01
10	0.03	0.05	0.02	0.03	0.04	0.02
11	-0.56	0.04	0.02	-0.01	0.01	0.01

Table XIV. Expected values of integral harmonics in D4B magnets

A. Integral harmonics at 0.2 T in D4B magnets (Ver. 1.0)

n	$\langle b_n \rangle$	$\Delta(b_n)$	$\sigma(b_n)$	$\langle a_n \rangle$	$\Delta(a_n)$	$\sigma(a_n)$
2	0.08	0.77	0.28	-0.12	3.68	1.53
3	-9.92	5.52	1.95	-1.10	0.49	0.17
4	-0.05	0.20	0.08	0.13	1.15	0.42
5	0.64	0.83	0.40	0.18	0.16	0.06
6	-0.01	0.08	0.03	-0.03	0.54	0.15
7	-0.26	0.21	0.10	-0.09	0.07	0.02
8	-0.03	0.03	0.01	-0.01	0.15	0.05
9	0.14	0.13	0.04	0.02	0.03	0.01
10	0.03	0.05	0.02	0.02	0.05	0.02
11	-0.66	0.04	0.02	-0.01	0.02	0.01

B. Integral harmonics at 3.55 T in D4B magnets (Ver. 1.0)

n	$\langle b_n \rangle$	$\Delta(b_n)$	$\sigma(b_n)$	$\langle a_n \rangle$	$\Delta(a_n)$	$\sigma(a_n)$
2	0.06	0.79	0.28	0.55	3.71	1.51
3	1.96	3.57	1.70	-1.07	0.55	0.18
4	-0.13	0.21	0.08	0.06	1.08	0.41
5	0.19	0.80	0.39	0.19	0.17	0.06
6	-0.03	0.10	0.04	0.00	0.55	0.16
7	0.02	0.19	0.10	-0.11	0.06	0.02
8	-0.01	0.03	0.01	-0.01	0.15	0.05
9	0.00	0.12	0.04	0.01	0.03	0.01
10	0.03	0.05	0.02	0.03	0.04	0.02
11	-0.56	0.04	0.02	-0.01	0.01	0.01

C. Integral harmonics at 3.8 T in D4B magnets (Ver. 1.0)

n	$\langle b_n \rangle$	$\Delta(b_n)$	$\sigma(b_n)$	$\langle a_n \rangle$	$\Delta(a_n)$	$\sigma(a_n)$
2	-0.07	0.79	0.28	0.53	3.71	1.51
3	1.99	3.57	1.70	-1.07	0.55	0.18
4	-0.21	0.21	0.08	0.05	1.08	0.41
5	0.04	0.80	0.39	0.19	0.17	0.06
6	-0.05	0.10	0.04	0.00	0.55	0.16
7	0.06	0.19	0.10	-0.10	0.06	0.02
8	-0.01	0.03	0.01	-0.01	0.15	0.05
9	0.00	0.12	0.04	0.01	0.03	0.01
10	0.03	0.05	0.02	0.03	0.04	0.02
11	-0.56	0.04	0.02	-0.01	0.01	0.01

7. Summary

Expected harmonics for BNL-built LHC dipoles are obtained by examining the vast amount of data in the RHIC DRG/DR8 magnets. A uniform procedure is adopted for all magnet types, starting from the warm straight section harmonics. POISSON calculations are used to estimate saturation effects where experimental data are not yet available. These calculations are preliminary at present and do not include all the sources of saturation. Also, locations of various holes etc. in the yoke are arbitrary at present. The tables of expected values will be revised when better calculations and/or experimental data are available.

Acknowledgement

The author would like to thank Peter Wanderer and Erich Willen for a critical review of the manuscript and many useful comments.

References

- [1] R. Gupta, R. Alforque, M. Anerella, E. Kelly, S. Plate, C. Rufer, P. Wanderer, E. Willen, and K. C. Wu, *Coldmass for LHC Dipole Insertion Magnets*, Proc. 15th International Conference on Magnet Technology (MT-15), Beijing, China, October 20-24, 1997.
- [2] R. Gupta, A. Jain, P. Wanderer, and E. Willen, *Magnetic Design of Dipoles for LHC Insertion Regions*, to be presented at the 6th European Particle Accelerator Conference (EPAC'98), Stockholm, June 22-26, 1998.